
Exploratory Diffusion Policy for Unsupervised Reinforcement Learning

Chengyang Ying¹ Huayu Chen¹ Xinning Zhou¹ Zhongkai Hao¹ Hang Su¹ Jun Zhu¹

Abstract

Unsupervised reinforcement learning (RL) aims to pre-train agents by exploring states or skills in reward-free environments, facilitating the adaptation to downstream tasks. However, existing methods often overlook the fitting ability of pre-trained policies and struggle to handle the heterogeneous pre-training data, which are crucial for achieving efficient exploration and fast fine-tuning. To address this gap, we propose Exploratory Diffusion Policy (EDP), which leverages the strong expressive ability of diffusion models to fit the explored data, both boosting exploration and obtaining an efficient initialization for downstream tasks. Specifically, we estimate the distribution of collected data in the replay buffer with the diffusion policy and propose a score intrinsic reward, encouraging the agent to explore unseen states. For fine-tuning the pre-trained diffusion policy on downstream tasks, we provide both theoretical analyses and practical algorithms, including an alternating method of Q function optimization and diffusion policy distillation. Extensive experiments demonstrate the effectiveness of EDP in efficient exploration during pre-training and fast adaptation during fine-tuning.

1. Introduction

Developing generalizable agents capable of efficiently adapting across various tasks remains a major challenge in reinforcement learning (RL). To address the diversity of downstream tasks, unsupervised learning has recently shown transformative progress in natural language processing (Brown et al., 2020) and computer vision (He et al., 2022), where pre-trained models can quickly adapt to different downstream tasks. Inspired by these successes, unsupervised RL (Eysenbach et al., 2018; Laskin et al., 2021)

aims to pre-train agents in reward-free environments, enabling them to fully extract embodiment knowledge. These pre-trained agents can then be fine-tuned for downstream tasks, characterized by task-specific rewards, with limited interactions.

One of the major challenges in unsupervised RL is the requirement of strong modeling ability and fitting ability for both the pre-training and fine-tuning stages. Specifically, to maximize exploration in reward-free environments during the pre-training stage, it requires designing intrinsic rewards that rely on an accurate estimation of the collected data distribution. This distribution is often heterogeneous, highlighting the importance of the modeling ability. As for the fine-tuning stage, the pre-trained policies need strong fitting ability to fully capture the diversity of the explored data, which is a critical factor for enabling rapid adaptation to downstream tasks (see Fig. 1). However, while existing unsupervised RL methods can collect diverse trajectories, they typically rely on simple pre-trained policies, such as Gaussian policies (Pathak et al., 2017; Mazzaglia et al., 2022) or skill-based policies (Eysenbach et al., 2018; Laskin et al., 2022), of which the expressive ability is always limited. Consequently, current pre-trained policies often fail to reflect the full diversity of the explored data in the replay buffer, hindering effective adaptation to downstream tasks.

To address above issues, we propose Exploratory Diffusion Policy (EDP), which leverages the strong modeling ability and the fitting ability of diffusion policies (Chen et al., 2023; Chi et al., 2023) to enhance unsupervised exploration and few-shot fine-tuning. During the unsupervised pre-training stage, we optimize a diffusion policy to estimate the heterogeneous distribution of the explored data in the replay buffer. As the diffusion policy can accurately estimate the data distribution, we propose a novel score intrinsic reward $\mathcal{R}_{\text{score}}$ calculated by the diffusion policy to encourage the agent to explore regions with lower probabilities in the replay buffer. To address the inefficiency of multi-step sampling in diffusion policies, we further adopt a Gaussian behavior policy for action generation during environment interaction. The behavior policy is optimized to maximize score intrinsic rewards and explore unseen regions.

Besides enabling accurate data estimation for intrinsic reward design, the pre-trained diffusion policy in EDP is also

^{*}Equal contribution ¹Department of Computer Science & Technology, Institute for AI, BNRist Center, Tsinghua-Bosch Joint ML Center, THBI Lab, Tsinghua University. Correspondence to: Jun Zhu <dcsczj@mail.tsinghua.edu.cn>.

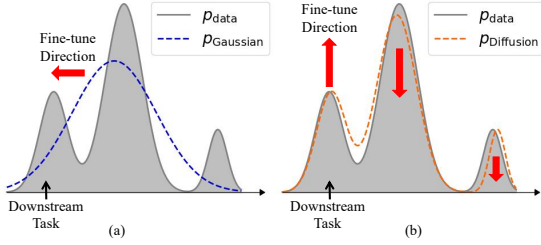


Figure 1. Illustration of different policies. (a) Gaussian policy struggles to fully fit the collected heterogeneous data and requires switching the probability mode to the mode of the downstream task, even if that mode has already been explored during pre-training. (b) Diffusion policy can fit all explored modes and only requires improving the probability of the mode of the downstream task.

an effective initialization for downstream tasks, as it can generate diverse trajectories based on exploration. During the fine-tuning stage, we provide a few-shot adaptation method with theoretical analyses. By alternately optimizing the Q function and the diffusion policy, our method fosters efficient adaptation to downstream tasks. The optimality of this approach is then proven in Theorem 3.1, following the analyses of soft RL (Haarnoja et al., 2017). In practice, to further improve the efficiency, we distill the score of the pre-trained diffusion policy along with the energy score of the guidance calculated by contrastive energy prediction (Lu et al., 2023), to derive the fine-tuned diffusion policy.

We evaluate the effectiveness of EDP in terms of both exploration and adaptation with various benchmarks, including Maze2d (Campos et al., 2020) and continuous control in URLB (Laskin et al., 2022). Visualizations in Maze2d demonstrate that EDP achieves a significantly larger state coverage ratio during the pre-training stage compared to existing exploration and skill-based baselines, highlighting its superior exploration capability. Additionally, the pre-trained policies in EDP exhibit the highest diversity, outperforming commonly chosen Gaussian policies and skill-based policies. As for the fine-tuning performance, extensive experiments in URLB show that EDP can quickly adapt to downstream tasks, outperforming existing exploration methods.

In summary, the main contributions are as follows:

- We propose Exploratory Diffusion Policy (EDP) to enhance the unsupervised exploration efficiency through our score intrinsic rewards.
- Leveraging the strong expressive ability of diffusion policies, the pre-trained policies of EDP can accurately capture the diversity of explored data and serve as an effective initialization for downstream fine-tuning.
- We conduct extensive evaluations of EDP across various settings, demonstrating its capability to achieve efficient exploration and fast fine-tuning.

2. Background

2.1. Unsupervised Reinforcement Learning

Reinforcement learning (RL) always considers a Markov decision process (MDP) \mathcal{M} , which is represented as $\mathcal{M} = (\mathcal{S}, \mathcal{A}, \mathcal{P}, \mathcal{R}, \rho_0, \gamma)$ (Sutton & Barto, 2018). Here \mathcal{S} and \mathcal{A} denote the state and action spaces, respectively. For $\forall (s, a) \in \mathcal{S} \times \mathcal{A}$, $\mathcal{P}(\cdot|s, a)$ is a distribution on \mathcal{S} , representing the dynamic of \mathcal{M} , and $\mathcal{R}(s, a)$ is the extrinsic task reward function. ρ_0 is the initial state distribution and γ is the discount factor. For a given policy $\pi : \mathcal{S} \rightarrow \Delta(\mathcal{A})$, we define the discount state distribution of π at state s as $d_\pi(s) = (1 - \gamma) \sum_{t=0}^{\infty} [\gamma^t \mathcal{P}(s_t = s)]$. The objective of RL is to maximize the expected cumulative return of the policy π over the task \mathcal{R} , which can be computed as:

$$J(\pi) \triangleq \mathbb{E}_{\tau \sim \mathcal{M}, \pi} [\mathcal{R}(\tau)] = \frac{1}{1 - \gamma} \mathbb{E}_{s \sim d_\pi, a \sim \pi} [\mathcal{R}(s, a)]. \quad (1)$$

To boost the generalization capabilities of RL agents across various downstream tasks, unsupervised RL typically includes two stages: unsupervised pre-training and few-shot fine-tuning. During the first stage, the agent explores in the reward-free environment \mathcal{M}^c , i.e., \mathcal{M} without the reward function \mathcal{R} . To guide unsupervised exploration, we will design the intrinsic rewards \mathcal{R}_{int} to encourage the agent to explore diverse states and pre-train the policy π to maximize the intrinsic reward. Then during the fine-tuning stage, agents are required to adapt the pre-trained policy to handle the downstream task represented by the extrinsic task-specific reward \mathcal{R} , only through limited online interactions with the environment (like one-tenth or less of the pre-training steps).

2.2. Diffusion Policies

Recent studies have demonstrated that diffusion models (Sohl-Dickstein et al., 2015; Ho et al., 2020) excel at accurately representing heterogeneous behaviors in continuous control, particularly through the use of diffusion policies (Chen et al., 2023; Wang et al., 2023; Chi et al., 2023). Given state-action pairs (s, a) sampled from some unknown policy $\mu(a|s)$, diffusion policies first consider the forward diffusion process that gradually injects Gaussian noise into actions:

$$\mathbf{a}_t = \alpha_t \mathbf{a} + \sigma_t \epsilon, \quad t \in [0, 1], \quad (2)$$

here ϵ is the standard Gaussian distribution, and α_t, σ_t are pre-defined hyperparameters satisfying that when $t = 0$, we have $\mathbf{a}_t = \mathbf{a}$, and when $t = 1$, we have $\mathbf{a}_t \approx \epsilon$. For $\forall t \in [0, 1]$, we can define the marginal distribution of \mathbf{a}_t as

$$p_t(\mathbf{a}_t | \mathbf{s}, t) = \int \mathcal{N}(\mathbf{a}_t | \alpha_t \mathbf{a}, \sigma_t^2 \mathbf{I}) \mu(\mathbf{a} | \mathbf{s}) d\mathbf{a}. \quad (3)$$

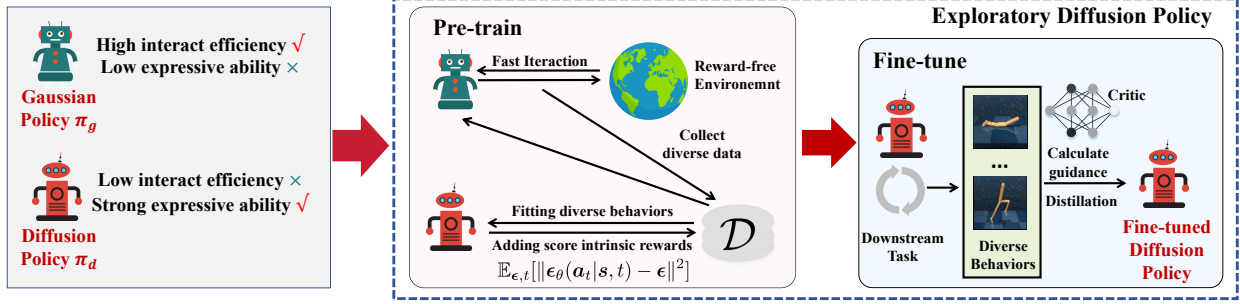


Figure 2. An overview of Exploratory Diffusion Policy (EDP). During pre-training, we employ the diffusion policy to model the heterogeneous exploration data and calculate score intrinsic rewards to further encourage exploration. Moreover, we adopt a Gaussian behavior policy to collect data that avoids the inefficiency caused by the multi-step sampling of the diffusion policy. In the fine-tuning stage for downstream tasks, we sample diverse behaviors from the pre-trained diffusion policy and then compute their energy guidance to distill an optimized fine-tuned diffusion policy.

Then diffusion policies will train a conditional “noise predictor” $\epsilon_\theta(\mathbf{a}_t|\mathbf{s}, t)$ to predict the added noise of each timestep:

$$\min_{\theta} \mathbb{E}_{t,\epsilon,\mathbf{s},\mathbf{a}} [||\epsilon_\theta(\mathbf{a}_t|\mathbf{s}, t) - \epsilon||^2]. \quad (4)$$

After training the conditional score estimator ϵ_θ , we can sample actions from diffusion policies to approximate the original policy $\mu(\mathbf{a}|\mathbf{s})$. In detail, we can discretize the corresponding diffusion ODEs of the reverse process (Song et al., 2021b) and sample with several numerical solvers (Song et al., 2021a; Lu et al., 2022) in around 5 ~ 15 steps.

3. Methodology

In this section, we will introduce Exploratory Diffusion Policy (EDP) during two stages: online unsupervised pre-training (Sec. 3.1) and online few-shot fine-tuning (Sec. 3.2).

3.1. Exploratory Diffusion Policy for Unsupervised Pre-training

During the unsupervised pre-training stage, existing methods mainly focus on designing intrinsic rewards to encourage Gaussian or skill-based policies to explore a wide range of states and skills. As discussed above, the core principle behind intrinsic rewards is to encourage the agent to visit state-action pairs that are less explored, i.e., those with low probabilities of occurrence in the replay buffer. Consequently, accurately estimating the distribution of the collected data in the replay buffer emerges as a promising pathway for calculating intrinsic rewards.

Based on the strong fitting ability of diffusion models, EDP leverages a diffusion policy π_d , represented by a parameterized score model ϵ_θ , to accurately model the diverse and often heterogeneous state-action pairs in the replay buffer \mathcal{D} collected before:

$$\min \mathbb{E}_{\mathbf{s},\mathbf{a} \sim \mathcal{D}} \mathbb{E}_{t,\epsilon} [||\epsilon_\theta(\mathbf{a}_t|\mathbf{s}, t) - \epsilon||^2]. \quad (5)$$

Then we can use $\log \pi_d(\mathbf{a}|\mathbf{s})$ to measure the frequency of an action being sampled in the replay buffer. Consequently, state-action pairs with low $\log \pi_d(\mathbf{a}|\mathbf{s})$ indicate they have been less explored. To encourage the agent to explore these regions, we design $-\log \pi_d(\mathbf{a}|\mathbf{s})$ as the intrinsic reward. Although estimating the log-probability of the diffusion policy is challenging, it is well known that $-\log \pi_d(\mathbf{a}|\mathbf{s})$ can be bounded by the following evidence lower bound (ELBO) (Ho et al., 2020):

$$-\log \pi_d(\mathbf{a}|\mathbf{s}) \leq \mathbb{E}_{\epsilon,t} [\mathbf{w}_t ||\epsilon_\theta(\mathbf{a}_t|\mathbf{s}, t) - \epsilon||^2] + C, \quad (6)$$

here C is a constant independent of θ , and \mathbf{w}_t are parameters related to α_t, σ_t , which are typically ignored (Ho et al., 2020). Consequently, our score intrinsic rewards are defined as the fitting loss of the diffusion policy:

$$\mathcal{R}_{\text{score}}(\mathbf{s}, \mathbf{a}) = \mathbb{E}_{\epsilon,t} [||\epsilon_\theta(\mathbf{a}_t|\mathbf{s}, t) - \epsilon||^2]. \quad (7)$$

Intuitively, score intrinsic rewards can measure the fitting quality of diffusion policy to the state-action pairs, thereby encouraging the agent to explore regions that are poorly fitted or unexplored. By maximizing these intrinsic rewards, EDP trains agents to discover unseen regions effectively. However, directly using diffusion policies to interact with reward-free environments during pre-training is inefficient and unstable due to the requirement of multi-step sampling. To address this issue, EDP incorporates a Gaussian behavior policy π_g to sample actions for fast and efficient interaction. The Gaussian behavior policy π_g can then be trained using any RL algorithm, guided by the score intrinsic reward $\mathcal{R}_{\text{score}}(\mathbf{s}, \mathbf{a})$. This encourages the exploration of regions where the diffusion policy either fits poorly or has not yet been exposed. Additionally, EDP is flexible to combine with existing unsupervised pre-training methods like ICM (Pathak et al., 2017) or RND (Burda et al., 2018) to further boost exploration. The pseudo code of the unsupervised exploration stage of EDP is in Algorithm 1.

Algorithm 1 Pre-training of EDP

Require: Reward-free environment \mathcal{M}^c , replay buffer \mathcal{D} , Gaussian behavior policy π_g , diffusion policy π_d parameterized with the score model ϵ_θ .

- 1: **for** sample step = 1, 2, ..., S **do**
- 2: **for** update step = 1, 2, ..., U **do**
- 3: Sample s - a pairs $\{(s^m, a^m)\}_{m=1}^M$ from \mathcal{D} .
- 4: Update ϵ_θ via optimizing with Eq. (5) with sampled data.
- 5: Calculate the score intrinsic rewards r^m via Eq. (7) for each sampled pair (s^m, a^m) .
- 6: Train π_g with (s^m, a^m, r^m) by any RL algorithm.
- 7: **end for**
- 8: Utilize the Gaussian behavior policy π_g to interact with \mathcal{M}^c and store state-action pairs into \mathcal{D} .
- 9: **end for**

3.2. Online Fine-tuning Exploratory Diffusion Policy

After obtaining the pre-trained diffusion policy π_d , the fine-tuning stage requires adapting π_d efficiently to handle the downstream task, represented by \mathcal{R} , by interacting with the environment within a limited number of timesteps. Existing unsupervised RL methods always directly apply online RL algorithms, such as DDPG (Lillicrap, 2015) or PPO (Schulman et al., 2017), for fine-tuning, which may be inefficient for EDP as the diffusion policy as the log probability is difficult to estimate. Below, we start by analyzing the objective of the fine-tuning stage in unsupervised RL and then design online fine-tuning algorithms for pre-trained diffusion policies. Given the limited iteration timesteps in the fine-tuning stage, the objective can be formulated as the combination of maximizing the cumulative return as well as keeping close to the pre-trained policy over every state s (Eysenbach et al., 2021; Ying et al., 2024):

$$\begin{aligned} \max_{\pi} J_f(\pi) &\triangleq J(\pi) - \frac{\beta}{(1-\gamma)} \mathbb{E}_{s \sim d_{\pi}} [D_{\text{KL}}(\pi(\cdot|s) \|\pi_d(\cdot|s))] \\ &= \frac{1}{1-\gamma} \mathbb{E}_{s \sim d_{\pi}, a \sim \pi} [\mathcal{R}(s, a) - \beta D_{\text{KL}}(\pi(\cdot|s) \|\pi_d(\cdot|s))] \\ &= \frac{1}{1-\gamma} \mathbb{E}_{s \sim d_{\pi}, a \sim \pi} \left[\mathcal{R}(s, a) - \beta \log \frac{\pi(a|s)}{\pi_d(a|s)} \right], \end{aligned} \quad (8)$$

here $\beta > 0$ is an unknown trade-off parameter that is related to the fine-tuning steps. The objective $J_f(\pi)$ can be interpreted as penalizing the probability offset of the policy in (s, a) over π and π_d . More specifically, it aims to maximize a surrogate reward of the form $\mathcal{R}(s, a) - \beta \log \frac{\pi(a|s)}{\pi_d(a|s)}$. Unfortunately, this surrogate reward depends on the policy π and we cannot directly apply classical MDP analyses. Drawn inspiration from soft RL (Haarnoja et al., 2017; 2018) and offline RL (Peng et al., 2019), we begin by defining the

Algorithm 2 Fine-tuning of EDP

Require: Environment \mathcal{M} with rewards \mathcal{R} , replay buffer \mathcal{D} , pre-trained diffusion policy π_d parameterized with the score model ϵ_θ , fine-tuned diffusion policy ϵ_ψ .

- 1: **for** update iteration $n = 1, 2, \dots, N$ **do**
- 2: Sample s - a - r pairs $\{(s^m, a^m, r^m)\}_{m=1}^M$ from \mathcal{D} .
- 3: Update Q function with IQM.
- 4: Update Guidance $f_{\phi_{n-1}}$ with CEP.
- 5: Optimize ψ by score distillation with Eq. 13.
- 6: **for** interaction step = 1, 2, ..., S **do**
- 7: Utilize the fine-tuned diffusion policy to interact with \mathcal{M} and store state-action-reward pairs into \mathcal{D} .
- 8: **end for**
- 9: **end for**

corresponding Q functions as follows:

$$\begin{aligned} Q_{\pi}(s, a) &= \mathbb{E} [\mathcal{R}(s, a) \\ &\quad + \sum_{i=1}^{\infty} \gamma^i \left(\mathcal{R}(s_i, a_i) - \beta \log \frac{\pi(a_i|s_i)}{\pi_d(a_i|s_i)} \right)]. \end{aligned} \quad (9)$$

Based on this Q function, we can simplify J_f as

$$J_f(\pi) = \mathbb{E}_{s \sim \rho_0, a \sim \pi} [Q_{\pi}(s, a) - \beta D_{\text{KL}}(\pi(\cdot|s) \|\pi_d(\cdot|s))]. \quad (10)$$

To maximize Eq. 10, EDP considers decoupling the optimization of the Q function and the diffusion policy with an alternating optimization method. In detail, we first initial $\pi_0 = \pi_d, Q_0 = Q_{\pi_0}$, then for $n = 1, 2, \dots$, we obtain

$$\begin{aligned} \pi_n(\cdot|s) &= \arg \max_{\pi} \mathbb{E}_{a \sim \pi} [Q_{\pi_{n-1}}(s, a) \\ &\quad - \beta D_{\text{KL}}(\pi(\cdot|s) \|\pi_d(\cdot|s))] \\ &= \frac{1}{Z(s)} \pi_d(a|s) e^{Q_{\pi_{n-1}}(s, a) / \beta}, \\ Q_n &= Q_{\pi_n}, \end{aligned} \quad (11)$$

here $Z(s) = \int \pi_d(a|s) e^{\beta Q_n(s, a)} da$ is the partition function. Building on the analyses of soft RL (Haarnoja et al., 2017; 2018), we can demonstrate that each iteration improves the policy’s performance and the alternating optimization will finally converge to the optimal policy of $J_f(\pi)$.

Theorem 3.1 (Proof in Appendix A). *The alternating optimization of EDP can achieve policy improvement, i.e., $J_f(\pi_n) \geq J_f(\pi_{n-1})$ holds for every $n \geq 1$. And π_n will converge to the optimal policy of J_f .*

Below we will introduce the practical fine-tuning algorithm of EDP for both updating the Q function and the diffusion policy respectively, with the pseudo-code in Algorithm 2.

Q function optimization. The core principle for updating our Q functions is to penalize actions of which the gap between the log probability of π and π_d is large. Consequently, we apply implicit Q-learning (IQL) (Kostrikov et al., 2022), which leverages expectile regression to penalize out-of-distribution actions (details are in Appendix B.1).

Diffusion policy fine-tune. At each update iteration n , given the Q function Q_{n-1} , it is difficult to directly calculate π_n by Eq. 11 as $Z(s)$ is a complicated integral. However, sampling from π_n can be regarded as sampling from an original diffusion model π_d with the energy guidance Q_{n-1} , which has been widely discussed as guided sampling (Chung et al., 2022; Janner et al., 2022; Lu et al., 2023). Especially, we employ contrastive energy prediction (CEP) (Lu et al., 2023) to sample from $\propto \pi_d e^{Q_{n-1}/\beta}$, which performs well in both image generation and offline RL. In detail, CEP will parameterize $f_{\phi_{n-1}}(s, \mathbf{a}_t, t)$ to represent the energy guidance of timestep t and its optimization follows:

$$\min_{\phi_{n-1}} \mathbb{E}_{t, \mathbf{s}} \mathbb{E}_{\mathbf{a}^1, \dots, \mathbf{a}^K \sim \pi_d(\cdot | \mathbf{s})} \left[- \sum_{i=1}^K \frac{e^{Q_{n-1}(s, \mathbf{a}^i)/\beta}}{\sum_{j=1}^K e^{Q_{n-1}(s, \mathbf{a}^j)/\beta}} \log \frac{f_{\phi_{n-1}}(s, \mathbf{a}_t^i, t)}{\sum_{j=1}^K f_{\phi_{n-1}}(s, \mathbf{a}_t^j, t)} \right]. \quad (12)$$

Then EDP fine-tunes the diffusion policy by distilling the score of π_{n+1} , which is parameterized as $\epsilon_\psi(\mathbf{a}_t | \mathbf{s}, t)$:

$$\min_{\psi} \mathbb{E}_{\mathbf{s}, \mathbf{a}, t} \|\epsilon_\psi(\mathbf{a}_t | \mathbf{s}, t) - \epsilon_\theta(\mathbf{a}_t | \mathbf{s}, t) - f_{\phi_{n-1}}(s, \mathbf{a}_t, t)\|^2. \quad (13)$$

Finally, ϵ_ψ is the estimated score function of π_n , and we can directly sample ϵ_ψ to generate action of π_n (details are in Appendix B.2).

4. Related Work

Unsupervised Pre-training in RL. To enhance the generalization ability of agents across various tasks, unsupervised RL focuses on pre-train agents in reward-free environments to acquire embodiment knowledge, which can later be fine-tuned to any downstream tasks. During the pre-training stage, existing methods mainly concentrate on designing intrinsic rewards to encourage agents to explore the environment, which can be mainly categorized into two types: exploration and skill discovery. Exploration methods typically train a simple Gaussian policy to explore diverse states by maximizing the intrinsic rewards designed to estimate either uncertainty (Pathak et al., 2017; Burda et al., 2018; Pathak et al., 2019; Mazzaglia et al., 2022; Ying et al., 2024) or state entropy (Lee et al., 2019; Liu & Abbeel, 2021b;a). Differently, skill-discovery methods hope to explore diverse

skills for downstream tasks, by maximizing the mutual information of skills and states (Eysenbach et al., 2018; Lee et al., 2019; Campos et al., 2020; Kim et al., 2021; Park et al., 2022; Laskin et al., 2022; Zhao et al., 2022; Yang et al., 2023; Park et al., 2023; Bai et al., 2024). However, existing methods primarily focus on collecting diverse states while neglecting the expression ability of the pre-trained policies. Specifically, although exploration methods can discover diverse trajectories, the pre-trained policy, which is always a simple Gaussian policy, exhibits unimodally and fails to capture the diversity present in the explored data. Similarly, skill-based policies typically consider discrete skill space with limited skills (Eysenbach et al., 2018), constraining their expressive ability by the predefined skill count. Moreover, skill-based methods always randomly select a fixed skill for adapting the downstream tasks (Yang et al., 2023), which degenerates into an unimodal Gaussian distribution, further limiting its expressive power. Consequently, the application of generative models with strong expressive ability for improving the diversity of pre-trained policies is still less studied.

RL with Diffusion Models. Recent advancements have demonstrated that diffusion models, with their strong expressive capabilities, can benefit RL from different perspectives (Zhu et al., 2023). In offline RL, diffusion policies (Wang et al., 2023; Chen et al., 2023; Chi et al., 2023; Hansen-Estruch et al., 2023; Kang et al., 2024; Chen et al., 2024c) have shown remarkable progress in modeling multimodal behaviors under the heterogeneous data distribution, outperforming previous policies such as Gaussians or VAEs. Besides policies, diffusion planners (Janner et al., 2022; Ajay et al., 2023; He et al., 2023; Liang et al., 2023; Chen et al., 2024a) have demonstrated the potential of diffusion models in long-term sequence prediction and test-time planning. Additionally, an array of research has explored integrating energy guidance into diffusion policies for guided sampling (Janner et al., 2022; Lu et al., 2023; Liu et al., 2024). In online RL, several works have investigated training diffusion policies online for improving the sample efficiency and performance (Psenka et al., 2023; Li et al., 2024; Ren et al., 2024; Mark et al., 2024). However, the computational cost of multi-step sampling still remains a limiting factor for the efficiency of diffusion policies in online settings. In addition to behavior modeling, diffusion models have also been employed as world models (Alonso et al., 2024; Ding et al., 2024) augmented replay buffer (Lu et al., 2024; Wang et al., 2024), hierarchical RL (Li et al., 2023; Chen et al., 2024b), etc., which are beneficial in increasing sample efficiency in RL. To the best of our knowledge, this work represents the first attempt to leverage diffusion policies for unsupervised exploration, thanks to the strong multimodal expressive ability and the powerful data distribution estimation ability of diffusion policies.

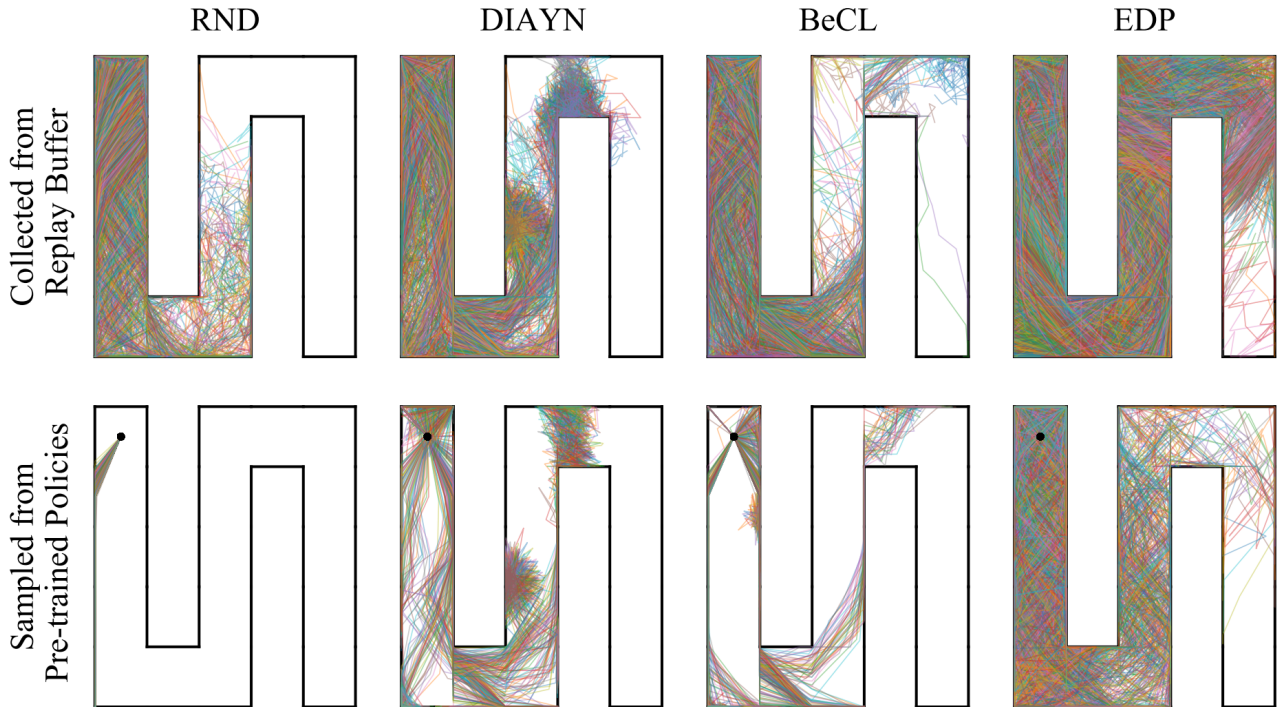


Figure 3. **Visualization of different unsupervised RL pre-training methods in Square-b maze.** The above part shows the trajectories in the replay buffer sampled by four algorithms during the unsupervised exploration stage. The below part visualizes the trajectories directly sampled from pre-trained policies of four algorithms.

5. Experiments

In this section, we present extensive empirical results to address the following questions:

- During the unsupervised pre-training stage, can EDP enhance exploration efficiency and obtain policies with diverse behaviors?
- Can the pre-trained policies of EDP fast adapt to downstream tasks?
- How do different components of EDP, like the score intrinsic reward, affect the performance?

5.1. Experimental Setup

Maze2d. We first conduct experiments for visualizing the diversity of collected trajectories during exploration and pre-trained policies in widely used maze2d environments (Campos et al., 2020; Yang et al., 2023). We choose 3 types of different mazes: Square-b, Square-c, and Square-tree. For all these mazes, the observations and actions both belong to \mathbb{R}^2 . When interacting with the mazes, the agents will be blocked when they contact the walls. We compare EDP with one exploration method: RND (Burda et al., 2018), as well

as two skill-discovery methods: DIAYN (Eysenbach et al., 2018) and BeCL (Yang et al., 2023), of which the skills are sampled from a 16-dimensional discrete distribution. For all methods, we pre-train agents in reward-free environments with 500k steps and store trajectories in the replay buffer. Then we visualize collected trajectories in the replay buffer as well as trajectories directly sampled by pre-trained policies. Moreover, to compare the exploration efficiency of different algorithms, we report their state coverage ratios in each maze during the pre-training stage, which are measured as the proportion of 0.01×0.01 square bins visited.

Continuous Control. To evaluate the fine-tuning performance in downstream tasks of pre-trained policies, we evaluate EDP in state-based continuous control settings of URLB (Laskin et al., 2021). In detail, we consider 4 different domains: Walker, Quadruped, Jaco, and Hopper. Each domain contains four downstream tasks. More details of these domains and downstream tasks are in Appendix C.1.

We compare EDP with 4 exploration baselines: ICM (Pathak et al., 2017), RND (Burda et al., 2018), Disagreement (Pathak et al., 2019), and LBS (Mazzaglia et al., 2022); as well as 5 skill discovery baselines: DIAYN (Eysenbach et al., 2018), SMM (Lee et al., 2019), LSD (Park et al., 2022), CIC (Laskin et al., 2022), and BeCL (Yang et al.,

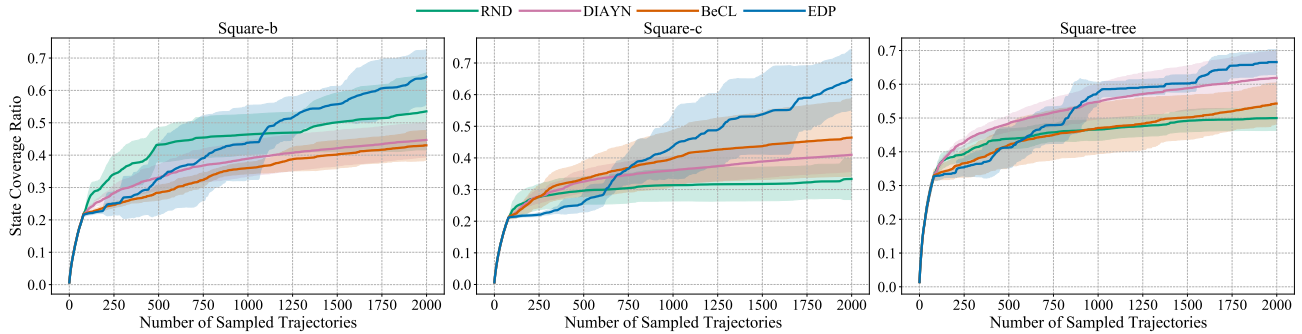


Figure 4. The state coverage ratios of different algorithms in Square-b, Square-c, and Square-tree in Maze2d during the pre-training stage.

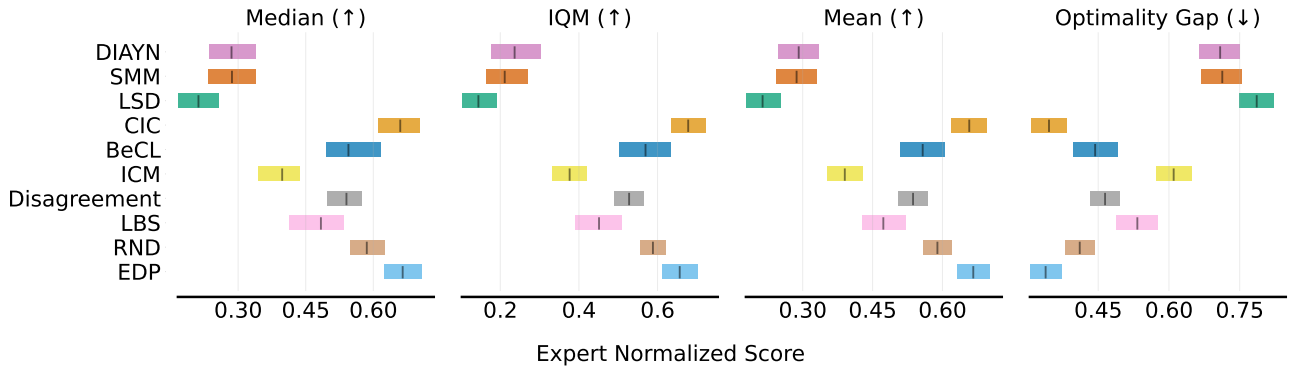


Figure 5. Aggregate metrics (Agarwal et al., 2021) in URLB. Each statistic for every algorithm has 160 runs (4 domains \times 4 downstream tasks \times 10 seeds).

2023), which are standard and SOTA in this benchmark. To enhance the exploration, we combine RDN rewards and our score intrinsic rewards in EDP. For all these baselines, we take DDPG (Sohl-Dickstein et al., 2015) as the RL backbone method, which is widely used in this benchmark. Following previous settings, for each algorithm, we first pre-train agents in the reward-free environment for 2M steps, and then fine-tune the pre-trained policy to adapt each downstream task with the extrinsic reward for 100K steps. All methods are run for 10 seeds per downstream task to mitigate the effectiveness of randomness caused by environments and policies.

5.2. Diversity of Pre-trained Policies

In Fig. 3, we visualize the trajectories collected during the unsupervised pre-training stage (upper part) and those directly sampled by the pre-trained policies (lower part) for each algorithm in the Square-b maze (the visualizations of other two mazes are in Appendix C.3). To quantitatively evaluate the exploration efficiency of each algorithm, we further compare their state coverage ratios as a function of the pre-training trajectory number and plot the curves of each maze in Fig. 4. On both the qualitative visualization and the

quantitative metric, EDP significantly outperforms existing methods, including exploration and skill-discovery ones, by large margins. These results demonstrate that our score intrinsic rewards, leveraging the accurate data estimation ability of diffusion models, effectively encourage agents to explore more diverse states during the unsupervised pre-training stage compared with baselines. Notably, while exploration-based methods like RND achieve state coverage comparable to skill-based methods, their pre-trained Gaussian policies often present an unimodal distribution near a single trajectory. In contrast, skill-based methods generate trajectories with greater diversity, as they rely on distinct skills sampled from a discrete distribution. However, this diversity is inherently limited by the number of predefined skills. Thanks to the strong expressive ability of diffusion models, the pre-trained diffusion policies of EDP can collect the most diverse trajectories compared with all baselines, which is significant for handling different downstream tasks.

5.3. Fine-tuning to Downstream Tasks

We now verify whether the policies pre-trained by EDP can fast adapt to downstream tasks in URLB. Following previous settings, for each downstream task, we train DDPG

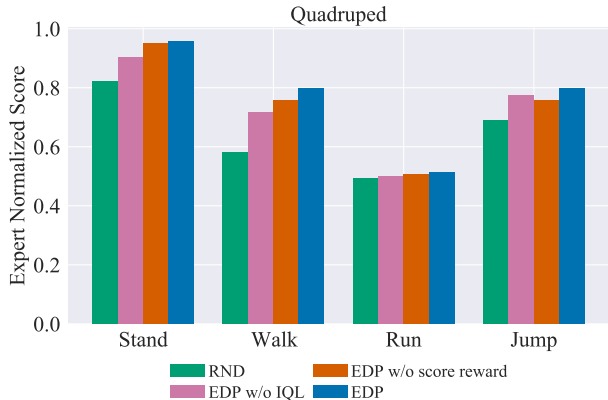


Figure 6. Ablation studies on score intrinsic reward and Q learning choices. EDP w/o score reward only utilizes RND reward rather than the score intrinsic reward for pre-training. EDP w/o IQL utilizes in-sample Q learning rather than IQL during fine-tuning.

agents with 2M steps to get the expert return and calculate the expert normalized score for each algorithm. Following previous work (Agarwal et al., 2021), in Fig. 5, we compare all methods with four metrics: mean, median, interquartile mean (IQM), and optimality gap (OG), along with stratified bootstrap confidence intervals. As shown here, EDP significantly outperforms all existing exploration methods such as RND and achieves competitive performance with SOTA skill-based methods such as CIC. Additional details and analyses are in Appendix C.4.

5.4. Ablation Studies

Score intrinsic rewards. We begin by conducting the ablation study on EDP during the pre-training stage, focusing on the choice of diffusion policy and the impact of our score intrinsic rewards. In detail, we design a variant, EDP w/o score reward, which is the same as EDP but removes our score intrinsic reward and only uses RND reward as the intrinsic reward. As shown in Fig. 6, for all four tasks in the quadruped domain, the performance of EDP w/o score reward is better than RND. This indicates that incorporating diffusion policies during pre-training effectively enhances policy diversity and benefits downstream task performance. Moreover, EDP consistently outperforms EDP w/o score reward, underscoring the effectiveness of our score intrinsic reward in improving fine-tuning outcomes.

Q function optimization. Additionally, we conduct an ablation study to evaluate the impact of different Q learning methods during the fine-tuning stage. In detail, we introduce EDP w/o IQL, which utilizes In-support Softmax Q-Learning (Lu et al., 2023) rather than IQL for the Q function optimization. The results, presented in Fig. 6, demonstrate that EDP consistently outperforms EDP w/o IQL, verifying the efficiency of IQL in fine-tuning the diffusion policies.

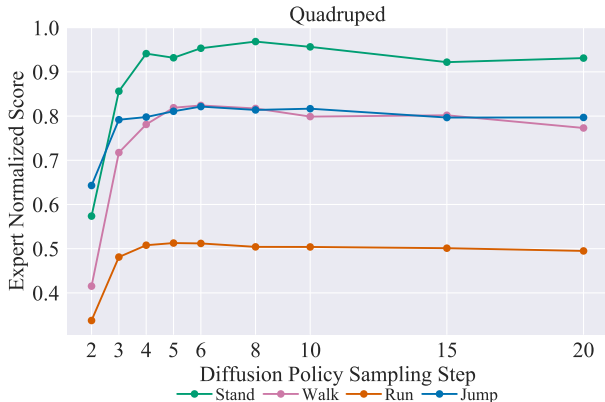


Figure 7. Ablation study on the diffusion steps for sampling actions from the fine-tuned policy in downstream task evaluation.

Sampling steps of diffusion policies. As mentioned above, to avoid time costs caused by the multi-step sampling of diffusion policies, our pre-training stage utilizes the behavior Gaussian policy to interact with the environment. During fine-tuning, EDP requires sampling actions from the diffusion policy for both trajectory generation and final evaluation. To accelerate this process, we adopt DPM-Solver (Lu et al., 2022) for faster sampling. For trajectory collection, we set the diffusion step to 15, following established offline RL settings (Lu et al., 2023). Additionally, we conduct an ablation study about the relationship between the performance of fine-tuned policies and the number of diffusion steps used during inference. The results, illustrated in Fig. 7, show that across all four tasks, performance improves as the number of diffusion steps increases and gradually stabilizes when the sampling step exceeds 5.

6. Conclusion

Unsupervised exploration is one of the major problems in RL for boosting agent generalization across tasks, as it relies on accurate intrinsic rewards to guide the exploration of unseen regions. In this work, we address the challenge of limited policy expressivity in previous exploration methods by leveraging the powerful expressive ability of diffusion policies. In detail, our Exploratory Diffusion Policy (EDP) not only enhances exploration efficiency during pre-training but also yields pre-trained policies with significant behavioral diversity. Furthermore, we provide a theoretical analysis of the fine-tuning stage for diffusion policies with practical alternating optimization methods. Experimental results in various settings demonstrate that EDP can effectively benefit both pre-training exploration and fine-tuning performance. We hope this work can inspire further research in developing high-fidelity generative models for improving unsupervised exploration, particularly in large-scale cross-embodiment pre-trained agents or real-world control applications.

Broader Impact

Designing generalizable agents for varying tasks is one of the major concerns in reinforcement learning. This work focuses on utilizing diffusion policies for exploration and proposes a novel algorithm EDP. One of the potential negative impacts is that algorithms mainly use deep neural networks, which lack interoperability and may face robustness issues. There are no serious ethical issues as this is basic research.

References

- Agarwal, R., Schwarzer, M., Castro, P. S., Courville, A. C., and Bellemare, M. Deep reinforcement learning at the edge of the statistical precipice. *Advances in neural information processing systems*, 34:29304–29320, 2021.
- Ajay, A., Du, Y., Gupta, A., Tenenbaum, J. B., Jaakkola, T. S., and Agrawal, P. Is conditional generative modeling all you need for decision making? In *The Eleventh International Conference on Learning Representations*, 2023. URL <https://openreview.net/forum?id=sP1fo2K9DFG>.
- Alonso, E., Jelley, A., Micheli, V., Kanervisto, A., Storkey, A., Pearce, T., and Fleuret, F. Diffusion for world modeling: Visual details matter in atari. *arXiv preprint arXiv:2405.12399*, 2024.
- Bai, C., Yang, R., Zhang, Q., Xu, K., Chen, Y., Xiao, T., and Li, X. Constrained ensemble exploration for unsupervised skill discovery. *arXiv preprint arXiv:2405.16030*, 2024.
- Brown, T., Mann, B., Ryder, N., Subbiah, M., Kaplan, J. D., Dhariwal, P., Neelakantan, A., Shyam, P., Sastry, G., Askell, A., et al. Language models are few-shot learners. *Advances in neural information processing systems*, 33:1877–1901, 2020.
- Burda, Y., Edwards, H., Storkey, A., and Klimov, O. Exploration by random network distillation. In *International Conference on Learning Representations*, 2018.
- Campos, V., Trott, A., Xiong, C., Socher, R., Giró-i Nieto, X., and Torres, J. Explore, discover and learn: Unsupervised discovery of state-covering skills. In *International Conference on Machine Learning*, pp. 1317–1327. PMLR, 2020.
- Chen, B., Monso, D. M., Du, Y., Simchowitz, M., Tedrake, R., and Sitzmann, V. Diffusion forcing: Next-token prediction meets full-sequence diffusion. *arXiv preprint arXiv:2407.01392*, 2024a.
- Chen, C., Deng, F., Kawaguchi, K., Gulcehre, C., and Ahn, S. Simple hierarchical planning with diffusion. *arXiv preprint arXiv:2401.02644*, 2024b.
- Chen, H., Lu, C., Ying, C., Su, H., and Zhu, J. Offline reinforcement learning via high-fidelity generative behavior modeling. In *The Eleventh International Conference on Learning Representations*, 2023. URL <https://openreview.net/forum?id=42zs3qa2kpy>.
- Chen, H., Zheng, K., Su, H., and Zhu, J. Aligning diffusion behaviors with q-functions for efficient continuous control. *arXiv preprint arXiv:2407.09024*, 2024c.
- Chi, C., Xu, Z., Feng, S., Cousineau, E., Du, Y., Burchfiel, B., Tedrake, R., and Song, S. Diffusion policy: Visuomotor policy learning via action diffusion. *The International Journal of Robotics Research*, pp. 02783649241273668, 2023.
- Chung, H., Kim, J., Mccann, M. T., Klasky, M. L., and Ye, J. C. Diffusion posterior sampling for general noisy inverse problems. *arXiv preprint arXiv:2209.14687*, 2022.
- Ding, Z., Zhang, A., Tian, Y., and Zheng, Q. Diffusion world model. *arXiv preprint arXiv:2402.03570*, 2024.
- Eysenbach, B., Gupta, A., Ibarz, J., and Levine, S. Diversity is all you need: Learning skills without a reward function. In *International Conference on Learning Representations*, 2018.
- Eysenbach, B., Salakhutdinov, R., and Levine, S. The information geometry of unsupervised reinforcement learning. In *International Conference on Learning Representations*, 2021.
- Haarnoja, T., Tang, H., Abbeel, P., and Levine, S. Reinforcement learning with deep energy-based policies. In *International conference on machine learning*, pp. 1352–1361. PMLR, 2017.
- Haarnoja, T., Zhou, A., Abbeel, P., and Levine, S. Soft actor-critic: Off-policy maximum entropy deep reinforcement learning with a stochastic actor. In *International conference on machine learning*, pp. 1861–1870. PMLR, 2018.
- Hansen-Estruch, P., Kostrikov, I., Janner, M., Kuba, J. G., and Levine, S. Idql: Implicit q-learning as an actor-critic method with diffusion policies. *arXiv preprint arXiv:2304.10573*, 2023.
- He, H., Bai, C., Xu, K., Yang, Z., Zhang, W., Wang, D., Zhao, B., and Li, X. Diffusion model is an effective planner and data synthesizer for multi-task reinforcement learning. *Advances in neural information processing systems*, 36:64896–64917, 2023.
- He, K., Chen, X., Xie, S., Li, Y., Dollár, P., and Girshick, R. Masked autoencoders are scalable vision learners. In *Proceedings of the IEEE/CVF conference on computer vision and pattern recognition*, pp. 16000–16009, 2022.

- Ho, J., Jain, A., and Abbeel, P. Denoising diffusion probabilistic models. *Advances in neural information processing systems*, 33:6840–6851, 2020.
- Janner, M., Du, Y., Tenenbaum, J., and Levine, S. Planning with diffusion for flexible behavior synthesis. In *International Conference on Machine Learning*, pp. 9902–9915. PMLR, 2022.
- Kang, B., Ma, X., Du, C., Pang, T., and Yan, S. Efficient diffusion policies for offline reinforcement learning. *Advances in Neural Information Processing Systems*, 36, 2024.
- Kim, J., Park, S., and Kim, G. Unsupervised skill discovery with bottleneck option learning. In *International Conference on Machine Learning*, pp. 5572–5582. PMLR, 2021.
- Kostrikov, I., Nair, A., and Levine, S. Offline reinforcement learning with implicit q-learning. In *International Conference on Learning Representations*, 2022. URL <https://openreview.net/forum?id=68n2s9ZJWF8>.
- Laskin, M., Yarats, D., Liu, H., Lee, K., Zhan, A., Lu, K., Cang, C., Pinto, L., and Abbeel, P. Urlb: Unsupervised reinforcement learning benchmark. In *Thirty-fifth Conference on Neural Information Processing Systems Datasets and Benchmarks Track (Round 2)*, 2021.
- Laskin, M., Liu, H., Peng, X. B., Yarats, D., Rajeswaran, A., and Abbeel, P. Unsupervised reinforcement learning with contrastive intrinsic control. *Advances in Neural Information Processing Systems*, 35:34478–34491, 2022.
- Lee, L., Eysenbach, B., Parisotto, E., Xing, E., Levine, S., and Salakhutdinov, R. Efficient exploration via state marginal matching. *arXiv preprint arXiv:1906.05274*, 2019.
- Li, W., Wang, X., Jin, B., and Zha, H. Hierarchical diffusion for offline decision making. In *International Conference on Machine Learning*, pp. 20035–20064. PMLR, 2023.
- Li, Z., Krohn, R., Chen, T., Ajay, A., Agrawal, P., and Chalvatzaki, G. Learning multimodal behaviors from scratch with diffusion policy gradient. *arXiv preprint arXiv:2406.00681*, 2024.
- Liang, Z., Mu, Y., Ding, M., Ni, F., Tomizuka, M., and Luo, P. Adaptdiffuser: Diffusion models as adaptive self-evolving planners. In *International Conference on Machine Learning*, pp. 20725–20745. PMLR, 2023.
- Lillicrap, T. Continuous control with deep reinforcement learning. *arXiv preprint arXiv:1509.02971*, 2015.
- Liu, H. and Abbeel, P. Aps: Active pretraining with successor features. In *International Conference on Machine Learning*, pp. 6736–6747. PMLR, 2021a.
- Liu, H. and Abbeel, P. Behavior from the void: Unsupervised active pre-training. *Advances in Neural Information Processing Systems*, 34:18459–18473, 2021b.
- Liu, X.-H., Liu, T.-S., Jiang, S., Chen, R., Zhang, Z., Chen, X., and Yu, Y. Energy-guided diffusion sampling for offline-to-online reinforcement learning. *arXiv preprint arXiv:2407.12448*, 2024.
- Lu, C., Zhou, Y., Bao, F., Chen, J., Li, C., and Zhu, J. Dpm-solver: A fast ode solver for diffusion probabilistic model sampling in around 10 steps. *Advances in Neural Information Processing Systems*, 35:5775–5787, 2022.
- Lu, C., Chen, H., Chen, J., Su, H., Li, C., and Zhu, J. Contrastive energy prediction for exact energy-guided diffusion sampling in offline reinforcement learning. In *International Conference on Machine Learning*, pp. 22825–22855. PMLR, 2023.
- Lu, C., Ball, P., Teh, Y. W., and Parker-Holder, J. Synthetic experience replay. *Advances in Neural Information Processing Systems*, 36, 2024.
- Mark, M. S., Gao, T., Sampaio, G. G., Srirama, M. K., Sharma, A., Finn, C., and Kumar, A. Policy agnostic rl: Offline rl and online rl fine-tuning of any class and backbone. *arXiv preprint arXiv:2412.06685*, 2024.
- Mazzaglia, P., Catal, O., Verbelen, T., and Dhoedt, B. Curiosity-driven exploration via latent bayesian surprise. In *Proceedings of the AAAI Conference on Artificial Intelligence*, volume 36, pp. 7752–7760, 2022.
- Park, S., Choi, J., Kim, J., Lee, H., and Kim, G. Lipschitz-constrained unsupervised skill discovery. In *International Conference on Learning Representations*, 2022.
- Park, S., Rybkin, O., and Levine, S. Metra: Scalable unsupervised rl with metric-aware abstraction. *arXiv preprint arXiv:2310.08887*, 2023.
- Pathak, D., Agrawal, P., Efros, A. A., and Darrell, T. Curiosity-driven exploration by self-supervised prediction. In *International conference on machine learning*, pp. 2778–2787. PMLR, 2017.
- Pathak, D., Gandhi, D., and Gupta, A. Self-supervised exploration via disagreement. In *International conference on machine learning*, pp. 5062–5071. PMLR, 2019.
- Peng, X. B., Kumar, A., Zhang, G., and Levine, S. Advantage-weighted regression: Simple and scalable off-policy reinforcement learning. *arXiv preprint arXiv:1910.00177*, 2019.

- Psenka, M., Escontrela, A., Abbeel, P., and Ma, Y. Learning a diffusion model policy from rewards via q-score matching. *arXiv preprint arXiv:2312.11752*, 2023.
- Ren, A. Z., Lidard, J., Ankile, L. L., Simeonov, A., Agrawal, P., Majumdar, A., Burchfiel, B., Dai, H., and Simchowitz, M. Diffusion policy optimization. *arXiv preprint arXiv:2409.00588*, 2024.
- Schulman, J., Wolski, F., Dhariwal, P., Radford, A., and Klimov, O. Proximal policy optimization algorithms. *arXiv preprint arXiv:1707.06347*, 2017.
- Sohl-Dickstein, J., Weiss, E., Maheswaranathan, N., and Ganguli, S. Deep unsupervised learning using nonequilibrium thermodynamics. In *International conference on machine learning*, pp. 2256–2265. PMLR, 2015.
- Song, J., Meng, C., and Ermon, S. Denoising diffusion implicit models. In *International Conference on Learning Representations*, 2021a. URL <https://openreview.net/forum?id=StlgiaRCHLP>.
- Song, Y., Sohl-Dickstein, J., Kingma, D. P., Kumar, A., Ermon, S., and Poole, B. Score-based generative modeling through stochastic differential equations. In *International Conference on Learning Representations*, 2021b. URL <https://openreview.net/forum?id=PXTIG12RRHS>.
- Sutton, R. S. and Barto, A. G. *Reinforcement learning: An introduction*. MIT press, 2018.
- Tassa, Y., Doron, Y., Muldal, A., Erez, T., Li, Y., Casas, D. d. L., Budden, D., Abdolmaleki, A., Merel, J., Lefrancq, A., et al. Deepmind control suite. *arXiv preprint arXiv:1801.00690*, 2018.
- Wang, R., Frans, K., Abbeel, P., Levine, S., and Efros, A. A. Prioritized generative replay. *arXiv preprint arXiv:2410.18082*, 2024.
- Wang, Z., Hunt, J. J., and Zhou, M. Diffusion policies as an expressive policy class for offline reinforcement learning. In *The Eleventh International Conference on Learning Representations*, 2023. URL <https://openreview.net/forum?id=AHvFDPi-FA>.
- Yang, R., Bai, C., Guo, H., Li, S., Zhao, B., Wang, Z., Liu, P., and Li, X. Behavior contrastive learning for unsupervised skill discovery. In *International Conference on Machine Learning*, pp. 39183–39204. PMLR, 2023.
- Ying, C., Zhou, X., Su, H., Yan, D., Chen, N., and Zhu, J. Towards safe reinforcement learning via constraining conditional value-at-risk. *arXiv preprint arXiv:2206.04436*, 2022.
- Ying, C., Hao, Z., Zhou, X., Xu, X., Su, H., Zhang, X., and Zhu, J. Peac: Unsupervised pre-training for cross-embodiment reinforcement learning. *arXiv preprint arXiv:2405.14073*, 2024.
- Zhao, A., Lin, M., Li, Y., Liu, Y.-J., and Huang, G. A mixture of surprises for unsupervised reinforcement learning. *Advances in Neural Information Processing Systems*, 35: 26078–26090, 2022.
- Zhu, Z., Zhao, H., He, H., Zhong, Y., Zhang, S., Guo, H., Chen, T., and Zhang, W. Diffusion models for reinforcement learning: A survey. *arXiv preprint arXiv:2311.01223*, 2023.

A. Theoretical analysis

Below we first analyze our fine-tuning objective Eq. 8 and then prove Theorem 3.1.

Assuming ρ_0 is the original state distribution of the MDP \mathcal{M} , we have

$$\begin{aligned}
 J_f(\pi) &\triangleq J(\pi) - \frac{\beta}{1-\gamma} \mathbb{E}_{\mathbf{s} \sim d_\pi} [D_{\text{KL}}(\pi(\cdot|\mathbf{s})\|\pi_d(\cdot|\mathbf{s}))] \\
 &= \frac{1}{1-\gamma} \mathbb{E}_{\mathbf{s} \sim d_\pi, \mathbf{a} \sim \pi(\cdot|\mathbf{s})} [\mathcal{R}(\mathbf{s}, \mathbf{a}) - \beta D_{\text{KL}}(\pi(\cdot|\mathbf{s})\|\pi_d(\cdot|\mathbf{s}))] \\
 &= \mathbb{E}_{\mathbf{s} \sim \rho_0, \mathbf{a} \sim \pi(\cdot|\mathbf{s})} \left[\sum_{i=0}^{\infty} \gamma^i (\mathcal{R}(\mathbf{s}_i, \mathbf{a}_i) - \beta D_{\text{KL}}(\pi(\cdot|\mathbf{s}_i)\|\pi_d(\cdot|\mathbf{s}_i))) \middle| \mathbf{s}_0 = \mathbf{s}, \mathbf{a}_0 = \mathbf{a} \right] \\
 &= \mathbb{E}_{\mathbf{s} \sim \rho_0, \mathbf{a} \sim \pi(\cdot|\mathbf{s})} \left[\mathcal{R}(\mathbf{s}, \mathbf{a}) - \beta D_{\text{KL}}(\pi(\cdot|\mathbf{s})\|\pi_d(\cdot|\mathbf{s})) + \sum_{i=1}^{\infty} \gamma^i (\mathcal{R}(\mathbf{s}_i, \mathbf{a}_i) - \beta D_{\text{KL}}(\pi(\cdot|\mathbf{s}_i)\|\pi_d(\cdot|\mathbf{s}_i))) \right] \\
 &= \mathbb{E}_{\mathbf{s} \sim \rho_0, \mathbf{a} \sim \pi(\cdot|\mathbf{s})} [Q_\pi(\mathbf{s}, \mathbf{a}) - \beta D_{\text{KL}}(\pi(\cdot|\mathbf{s})\|\pi_d(\cdot|\mathbf{s}))],
 \end{aligned} \tag{14}$$

here we set

$$\begin{aligned}
 Q_\pi(\mathbf{s}, \mathbf{a}) &= \mathbb{E} \left[\mathcal{R}(\mathbf{s}, \mathbf{a}) + \sum_{i=1}^{\infty} \gamma^i \left(\mathcal{R}(\mathbf{s}_i, \mathbf{a}_i) - \beta \log \frac{\pi(\mathbf{a}_i|\mathbf{s}_i)}{\pi_d(\mathbf{a}_i|\mathbf{s}_i)} \right) \right] \\
 &= \mathbb{E} \left[\mathcal{R}(\mathbf{s}, \mathbf{a}) + \sum_{i=1}^{\infty} \gamma^i (\mathcal{R}(\mathbf{s}_i, \mathbf{a}_i) - \beta D_{\text{KL}}(\pi(\cdot|\mathbf{s}_i)\|\pi_d(\cdot|\mathbf{s}_i))) \right].
 \end{aligned} \tag{15}$$

As discussed in Sec. 3.2, EDP applies the following alternative optimization method:

$$\begin{aligned}
 \pi_n(\cdot|\mathbf{s}) &= \arg \max_{\pi} \mathbb{E}_{\mathbf{a} \sim \pi(\cdot|\mathbf{s})} [Q_{\pi_{n-1}}(\mathbf{s}, \mathbf{a}) - \beta D_{\text{KL}}(\pi(\cdot|\mathbf{s})\|\pi_d(\cdot|\mathbf{s}))], \\
 Q_n &= Q_{\pi_n},
 \end{aligned} \tag{16}$$

Now we prove that $\pi_n(\mathbf{a}|\mathbf{s}) = \frac{1}{Z(\mathbf{s})} \pi_d(\mathbf{a}|\mathbf{s}) e^{Q_{n-1}(\mathbf{s}, \mathbf{a})/\beta}$. More generally, we define

$$F(\pi, \pi', \mathbf{s}) = \mathbb{E}_{\mathbf{a} \sim \pi(\cdot|\mathbf{s})} [Q_{\pi'}(\mathbf{s}, \mathbf{a}) - \beta D_{\text{KL}}(\pi(\cdot|\mathbf{s})\|\pi_d(\cdot|\mathbf{s}))]. \tag{17}$$

Using the calculus of variations, we can calculate the optimal point π^* of F satisfying that

$$Q_{\pi'}(\mathbf{s}, \mathbf{a}) = \beta \log \frac{\pi^*(\mathbf{a}|\mathbf{s})}{\pi_d(\mathbf{a}|\mathbf{s})} + b\beta, \tag{18}$$

here b is a constant not related to π^* , and we have $\pi^*(\mathbf{a}|\mathbf{s}) = \pi_d(\mathbf{a}|\mathbf{s}) e^{\frac{Q_{\pi'}(\mathbf{s}, \mathbf{a})}{\beta} - b}$. As $\int \pi^*(\mathbf{a}|\mathbf{s}) d\mathbf{a} = 1$, we can calculate that

$$b = \log \int \pi_d(\mathbf{a}|\mathbf{s}) e^{\frac{Q_{\pi'}(\mathbf{s}, \mathbf{a})}{\beta}} d\mathbf{a}, \quad \pi^*(\mathbf{a}|\mathbf{s}) = \frac{\pi_d(\mathbf{a}|\mathbf{s}) e^{\frac{Q_{\pi'}(\mathbf{s}, \mathbf{a})}{\beta} - b}}{\int \pi_d(\mathbf{a}|\mathbf{s}) e^{\frac{Q_{\pi'}(\mathbf{s}, \mathbf{a})}{\beta}} d\mathbf{a}}. \tag{19}$$

i.e., we have $\arg \max_{\pi} F(\pi, \pi', \mathbf{s}) \propto \pi_d(\cdot|\mathbf{s}) e^{Q_{\pi'}(\mathbf{s}, \cdot)/\beta}$ and thus $\pi_n(\mathbf{a}|\mathbf{s}) = \frac{1}{Z(\mathbf{s})} \pi_d(\mathbf{a}|\mathbf{s}) e^{Q_{n-1}(\mathbf{s}, \mathbf{a})/\beta}$.

Below we will prove Theorem 3.1.

Proof. Based on the definition of F , we have $J_f(\pi) = \mathbb{E}_{\mathbf{s} \sim \rho_0} F(\pi, \pi, \mathbf{s})$. Thus we require to prove $\mathbb{E}_{\mathbf{s} \sim \rho_0} F(\pi_n, \pi_n, \mathbf{s}) \geq \mathbb{E}_{\mathbf{s} \sim \rho_0} F(\pi_{n-1}, \pi_{n-1}, \mathbf{s})$. As we have discussed above,

$$\begin{aligned}
 \pi_n(\cdot|\mathbf{s}) &= \arg \max_{\pi} F(\pi, \pi_{n-1}, \mathbf{s}) = \frac{1}{Z(\mathbf{s})} \pi_d(\mathbf{a}|\mathbf{s}) e^{\beta Q_{\pi_{n-1}}(\mathbf{s}, \mathbf{a})}. \\
 F(\pi_n, \pi_{n-1}, \mathbf{s}) &\geq F(\pi_{n-1}, \pi_{n-1}, \mathbf{s}).
 \end{aligned} \tag{20}$$

In other words, we have proven that $\mathbb{E}_{\mathbf{s} \sim \rho_0} F(\pi_n, \pi_{n-1}, \mathbf{s}) \geq \mathbb{E}_{\mathbf{s} \sim \rho_0} F(\pi_{n-1}, \pi_{n-1}, \mathbf{s})$. Moreover, we have

$$\begin{aligned} Q_{\pi_{n-1}}(\mathbf{s}, \mathbf{a}) &= \mathcal{R}(\mathbf{s}, \mathbf{a}) + \mathbb{E} \left[\sum_{i=1}^{\infty} \gamma^i (\mathcal{R}(\mathbf{s}_i, \mathbf{a}_i) - \beta D_{\text{KL}}(\pi_{n-1}(\cdot | \mathbf{s}_i) \| \pi_d(\cdot | \mathbf{s}_i))) \middle| \mathbf{s}_0 = \mathbf{s}, \mathbf{a}_0 = \mathbf{a} \right] \\ &= \mathcal{R}(\mathbf{s}, \mathbf{a}) - \beta \gamma \mathbb{E}_{\mathbf{s}_1} (D_{\text{KL}}(\pi_{n-1}(\cdot | \mathbf{s}_1) \| \pi_d(\cdot | \mathbf{s}_1))) + \gamma \mathbb{E}_{\mathbf{s}_1, \mathbf{a}_1} [Q_{\pi_{n-1}}(\mathbf{s}_1, \mathbf{a}_1)] \\ &= \mathcal{R}(\mathbf{s}, \mathbf{a}) + \gamma \mathbb{E}_{\mathbf{s}_1} F(\pi_{n-1}, \pi_{n-1}, \mathbf{s}). \end{aligned} \quad (21)$$

Thus

$$\begin{aligned} & Q_{\pi_n}(\mathbf{s}, \mathbf{a}) - Q_{\pi_{n-1}}(\mathbf{s}, \mathbf{a}) \\ &= \gamma \mathbb{E}_{\mathbf{s}_1} [F(\pi_n, \pi_n, \mathbf{s}_1) - F(\pi_{n-1}, \pi_{n-1}, \mathbf{s}_1)] \geq \gamma \mathbb{E}_{\mathbf{s}_1} [F(\pi_n, \pi_n, \mathbf{s}_1) - F(\pi_n, \pi_{n-1}, \mathbf{s}_1)] \\ &= \gamma \mathbb{E}_{\mathbf{s}_1} \mathbb{E}_{\mathbf{a}_1 \sim \pi_n} [Q_{\pi_n}(\mathbf{s}_1, \mathbf{a}_1) - \beta D_{\text{KL}}(\pi_n(\cdot | \mathbf{s}_1) \| \pi_d(\cdot | \mathbf{s}_1)) - Q_{\pi_{n-1}}(\mathbf{s}_1, \mathbf{a}_1) + \beta D_{\text{KL}}(\pi_n(\cdot | \mathbf{s}_1) \| \pi_d(\cdot | \mathbf{s}_1))] \\ &= \gamma \mathbb{E}_{\mathbf{s}_1} \mathbb{E}_{\mathbf{a}_1 \sim \pi_n} [Q_{\pi_n}(\mathbf{s}_1, \mathbf{a}_1) - Q_{\pi_{n-1}}(\mathbf{s}_1, \mathbf{a}_1)]. \end{aligned} \quad (22)$$

Given the property of d_π that $d_\pi(\mathbf{s}) - (1 - \gamma)\rho_0(\mathbf{s}) = \gamma \sum_{\mathbf{s}'} d_\pi(\mathbf{s}') \sum_{\mathbf{a}} \pi(\mathbf{a} | \mathbf{s}') \mathcal{P}(\mathbf{s} | \mathbf{s}', \mathbf{a})$ (Ying et al., 2022), we have

$$\begin{aligned} & \mathbb{E}_{\mathbf{s} \sim d_{\pi_n}, \mathbf{a} \sim \pi_n(\cdot | \mathbf{s})} [Q_{\pi_n}(\mathbf{s}, \mathbf{a}) - Q_{\pi_{n-1}}(\mathbf{s}, \mathbf{a})] \\ & \geq \gamma \mathbb{E}_{\mathbf{s} \sim d_{\pi_n}, \mathbf{a} \sim \pi_n(\cdot | \mathbf{s})} \mathbb{E}_{\mathbf{s}_1} \mathbb{E}_{\mathbf{a}_1 \sim \pi_n} [Q_{\pi_n}(\mathbf{s}_1, \mathbf{a}_1) - Q_{\pi_{n-1}}(\mathbf{s}_1, \mathbf{a}_1)] \\ & = \int (d_{\pi_n}(\mathbf{s}_1) - (1 - \gamma)\rho_0(\mathbf{s}_1)) \mathbb{E}_{\mathbf{a}_1 \sim \pi_n} [Q_{\pi_n}(\mathbf{s}_1, \mathbf{a}_1) - Q_{\pi_{n-1}}(\mathbf{s}_1, \mathbf{a}_1)] d\mathbf{s}_1 \\ & = \mathbb{E}_{\mathbf{s}_1 \sim d_{\pi_n}, \mathbf{a}_1 \sim \pi_n(\cdot | \mathbf{s}_1)} [Q_{\pi_n}(\mathbf{s}_1, \mathbf{a}_1) - Q_{\pi_{n-1}}(\mathbf{s}_1, \mathbf{a}_1)] - (1 - \gamma) \mathbb{E}_{\mathbf{s}_1 \sim \rho_0, \mathbf{a}_1 \sim \pi_n(\cdot | \mathbf{s}_1)} [Q_{\pi_n}(\mathbf{s}_1, \mathbf{a}_1) - Q_{\pi_{n-1}}(\mathbf{s}_1, \mathbf{a}_1)]. \end{aligned} \quad (23)$$

Consequently,

$$\mathbb{E}_{\mathbf{s} \sim \rho_0} F(\pi_n, \pi_{n-1}, \mathbf{s}) - \mathbb{E}_{\mathbf{s} \sim \rho_0} F(\pi_{n-1}, \pi_{n-1}, \mathbf{s}) = \mathbb{E}_{\mathbf{s}_1 \sim \rho_0, \mathbf{a}_1 \sim \pi_n(\cdot | \mathbf{s}_1)} [Q_{\pi_n}(\mathbf{s}_1, \mathbf{a}_1) - Q_{\pi_{n-1}}(\mathbf{s}_1, \mathbf{a}_1)] \geq 0 \quad (24)$$

Finally, we have

$$J_f(\pi_n) = \mathbb{E}_{\mathbf{s} \sim \rho_0} F(\pi_n, \pi_n, \mathbf{s}) \geq \mathbb{E}_{\mathbf{s} \sim \rho_0} F(\pi_n, \pi_{n-1}, \mathbf{s}) \geq \mathbb{E}_{\mathbf{s} \sim \rho_0} F(\pi_{n-1}, \pi_{n-1}, \mathbf{s}) = J_f(\pi_{n-1}). \quad (25)$$

Thus our policy iteration can improve the performance. Moreover, under some regularity conditions, π_n converges to π_∞ . Since non-optimal policies can be improved by our iteration, the converged policy π_∞ is optimal for J_f . \square

B. Details of EDP

Below we discuss more details about the Q function optimization and diffusion policy optimization of EDP during the fine-tuning stage.

B.1. Q function optimization

For the Q function optimization, we choose to use implicit Q-learning (IQL) (Kostrikov et al., 2022), which is efficient to penalize out-of-distribution actions (Hansen-Estruch et al., 2023). The main training pipeline of IQL is expectile regression, i.e.,

$$\begin{aligned} \min_{\zeta} L_V(\zeta) &= \mathbb{E}_{\mathbf{s}, \mathbf{a} \sim \mathcal{D}} [L_2^\tau(Q_\phi(\mathbf{s}, \mathbf{a}) - V_\psi(\mathbf{s}))], \\ \min_{\phi} L_Q(\phi) &= \mathbb{E}_{\mathbf{s}, \mathbf{a}, \mathbf{s}' \sim \mathcal{D}} [\|r(\mathbf{s}, \mathbf{a}) + \gamma V_\zeta(\mathbf{s}') - Q_\phi(\mathbf{s}, \mathbf{a})\|^2], \end{aligned} \quad (26)$$

here $L_2^\tau(\mathbf{u}) = |\tau - \mathbf{1}(\mathbf{u} < 0)|\mathbf{u}^2$ and τ is a hyper-parameter. In detail, when $\tau > 0.5$, L_2^τ will downweight actions with low Q-values and give more weight to actions with larger Q-values.

B.2. Diffusion Policy Fine-tuning

For sampling from $\pi_n = \frac{1}{Z(\mathbf{s})} \pi_d e^{Q_{n-1}/\beta}$, we choose contrastive energy prediction (CEP) (Lu et al., 2023), a powerful guided sampling method. First, we calculate the score function of π_n as

$$\nabla_{\mathbf{a}} \log \pi_n(\mathbf{a}|\mathbf{s}) = \nabla_{\mathbf{a}} \log \pi_d(\mathbf{a}|\mathbf{s}) + \frac{1}{\beta} \nabla_{\mathbf{a}} Q_{n-1}(\mathbf{s}, \mathbf{a}). \quad (27)$$

Moreover, to calculate the score function of π_n at each timestep t , i.e., $\nabla_{\mathbf{a}_t} \log \pi_t^n(\mathbf{a}|\mathbf{s})$, CEP further defines the following Intermediate Energy Guidance:

$$\mathcal{E}_t^{n-1}(\mathbf{s}, \mathbf{a}_t) = \begin{cases} \frac{1}{\beta} Q_{n-1}(\mathbf{s}, \mathbf{a}_0), & t = 0 \\ \log \mathbb{E}_{\mu_{0t}(\mathbf{a}_0|\mathbf{s}, \mathbf{a}_t)} [e^{Q_{n-1}(\mathbf{s}, \mathbf{a}_0)/\beta}], & t > 0 \end{cases} \quad (28)$$

Then Theorem 3.1 in CEP proves that

$$\begin{aligned} \pi_t^n(\mathbf{a}_t|\mathbf{s}) &\propto \pi_d(\mathbf{a}_t|\mathbf{s}) e^{\mathcal{E}_t^{n-1}(\mathbf{s}, \mathbf{a}_t)}, \\ \nabla_{\mathbf{a}_t} \log \pi_t^n(\mathbf{a}_t|\mathbf{s}) &= \nabla_{\mathbf{a}_t} \log \pi_d(\mathbf{a}_t|\mathbf{s}) + \nabla_{\mathbf{a}_t} \mathcal{E}_t^{n-1}(\mathbf{s}, \mathbf{a}_t). \end{aligned} \quad (29)$$

For estimating $\nabla_{\mathbf{a}_t} \mathcal{E}_t^{n-1}(\mathbf{s}, \mathbf{a}_t)$, CEP considers a parameterized neural network $f_{\phi_{n-1}}(\mathbf{s}, \mathbf{a}_t, t)$ with the following objective:

$$\min_{\phi_{n-1}} \mathbb{E}_{t, \mathbf{s}} \mathbb{E}_{\mathbf{a}^1, \dots, \mathbf{a}^K \sim \pi_d(\cdot|\mathbf{s})} \left[- \sum_{i=1}^K \frac{e^{Q_{n-1}(\mathbf{s}, \mathbf{a}^i)/\beta}}{\sum_{j=1}^K e^{Q_{n-1}(\mathbf{s}, \mathbf{a}^j)/\beta}} \log \frac{f_{\phi_{n-1}}(\mathbf{s}, \mathbf{a}_t^i, t)}{\sum_{j=1}^K f_{\phi_{n-1}}(\mathbf{s}, \mathbf{a}_t^j, t)} \right]. \quad (30)$$

Then Theorem 3.2 in CEP has proven that its optimal solution $f_{\phi_{n-1}^*}$ satisfying that $\nabla_{\mathbf{a}_t} f_{\phi_{n-1}^*}(\mathbf{s}, \mathbf{a}_t, t) = \nabla_{\mathbf{a}_t} \mathcal{E}_t^{n-1}(\mathbf{s}, \mathbf{a}_t)$.

Consequently, we propose to fine-tune $\nabla_{\mathbf{a}_t} \log \pi_t^n(\mathbf{a}_t|\mathbf{s})$ parameterized as $\mathbf{s}_\psi(\mathbf{a}_t|\mathbf{s}, t)$ with the following distillation objective:

$$\min_{\psi} \mathbb{E}_{\mathbf{s}, \mathbf{a}, t} \|\epsilon_\psi(\mathbf{a}_t|\mathbf{s}, t) - \epsilon_\theta(\mathbf{a}_t|\mathbf{s}, t) - f_{\phi_{n-1}}(\mathbf{s}, \mathbf{a}_t, t)\|^2. \quad (31)$$

And the optimal solution ψ^* satisfying that $\epsilon_{\psi^*}(\mathbf{a}_t|\mathbf{s}, t)$ is the score function of π_n , i.e., we can sample from $\epsilon_{\psi^*}(\mathbf{a}_t|\mathbf{s}, t)$ with any unconditional diffusion model sampling methods like DDIM (Song et al., 2021a) or DPM-solver (Lu et al., 2022).

C. Experimental Details

In this section, we will introduce more about our experimental details. In Sec. C.1, we first introduce all the domains and tasks evaluated in our experiments. Then we briefly illustrate all the baselines compared in experiments in Sec. C.2. Moreover, we supplement more detailed experimental results about maze2d and URLB in Sec. C.3 and Sec. C.4, respectively.

Codes of EDP are provided in the Supplementary Material.

C.1. Domains and Tasks

Maze2d. This setting includes three kinds of mazes: Square-b, Square-c, and Square-tree. The visualization results in Square-b is in Fig. 3, and the visualization of other two mazes is in Appendix C.3.

Continuous Control. Our domains of continuous control follow URLB (Laskin et al., 2021), including 4 domains: Walker, Quadruped, Jaco, and Hopper, each with 4 downstream tasks from Deepmind Control Suite (DMC) (Tassa et al., 2018):

- **Walker** is a two-leg robot, including 4 downstream tasks: stand, walk, run, and flip.
- **Quadruped** is a quadruped robot within a 3D space, including 4 tasks: stand, walk, run, and jump.
- **Jaco** is a 6-DOF robotic arm with a 3-finger gripper, including 4 tasks: reach-top-left (tl), reach-top-right (tr), reach-bottom-left (bl), and reach-bottom-right (br).
- **Hopper** is a one-legged hopper robot, including 4 tasks: hop, hop-backward, flip, and flip-backward.

C.2. Baselines and Implementations

ICM (Pathak et al., 2017). Intrinsic Curiosity Module (ICM) trains a forward dynamics model and designs intrinsic rewards as the prediction error of the trained dynamics model.

RND (Burda et al., 2018). Random Network Distillation (RND) utilizes the error between the predicted features of a trained neural network and a fixed randomly initialized neural network as the intrinsic rewards.

Disagreement (Pathak et al., 2019) The Disagreement algorithm proposes a self-supervised algorithm that trains an ensemble of dynamics models and leverages the prediction variance between multiple models to estimate state uncertainty.

LBS (Mazzaglia et al., 2022). Latent Bayesian Surprise (LBS) designs the intrinsic reward as the Bayesian surprise within a latent space, i.e., the difference between prior and posterior beliefs of system dynamics.

DIAYN (Eysenbach et al., 2018). Diversity is All You Need (DIAYN) proposes to learn a diverse set of skills during the unsupervised pre-training stage, by maximizing the mutual information between states and skills.

SMM (Lee et al., 2019). State Marginal Matching (SMM) aims at learning a policy, of which the state distribution matches a given target state distribution.

LSD (Park et al., 2022). Lipschitz-constrained Skill Discovery (LSD) adopts a Lipschitz-constrained state representation function for maximizing the traveled distances of states and skills.

CIC (Laskin et al., 2022). Contrastive Intrinsic Control (CIC) leverages contrastive learning between state and skill representations, which can both learn the state representation and encourage behavioral diversity.

BeCL (Yang et al., 2023). Behavior Contrastive Learning (BeCL) defines intrinsic rewards as the mutual information (MI) between states sampled from the same skill, utilizing contrastive learning among behaviors.

In experiments of URLB, most baselines (ICM, RND, Disagreement, DIAYN, SMM) combined with RL backbone DDPG are directly following the official implementation in urlb (https://github.com/rll-research/url_benchmark). For LBS, we refer to the official implementation (<https://github.com/mazpie/mastering-urlb>) and combine

it with the codebase of urlb. For CIC and BeCL, we also follow their official implementations (<https://github.com/rll-research/cic>, <https://github.com/Rooshy-yang/BeCL>).

C.3. Additional Experiments in Maze

Moreover, we include the visualization of four algorithms (RND, DIAYN, BeCL, and EDP) in the other two mazes (square-c, square-tree) in Fig. 8 and Fig. 9, respectively. Similarly, in the above part of these two figures, we report all the trajectories sampled during the pre-training stage of each algorithm, while in the below part, we directly collect trajectories from the pre-trained policies.

As shown in these figures, although all four algorithms can explore unseen states and try to cover as many states as they can. Due to the limitation of the expressive ability, the behaviors of baselines can not fully cover the explored replay buffer. Differently, utilizing the strong modeling ability of diffusion models, the pre-trained policies of EDP can perform diverse behaviors, setting a great initialization for handling downstream tasks.

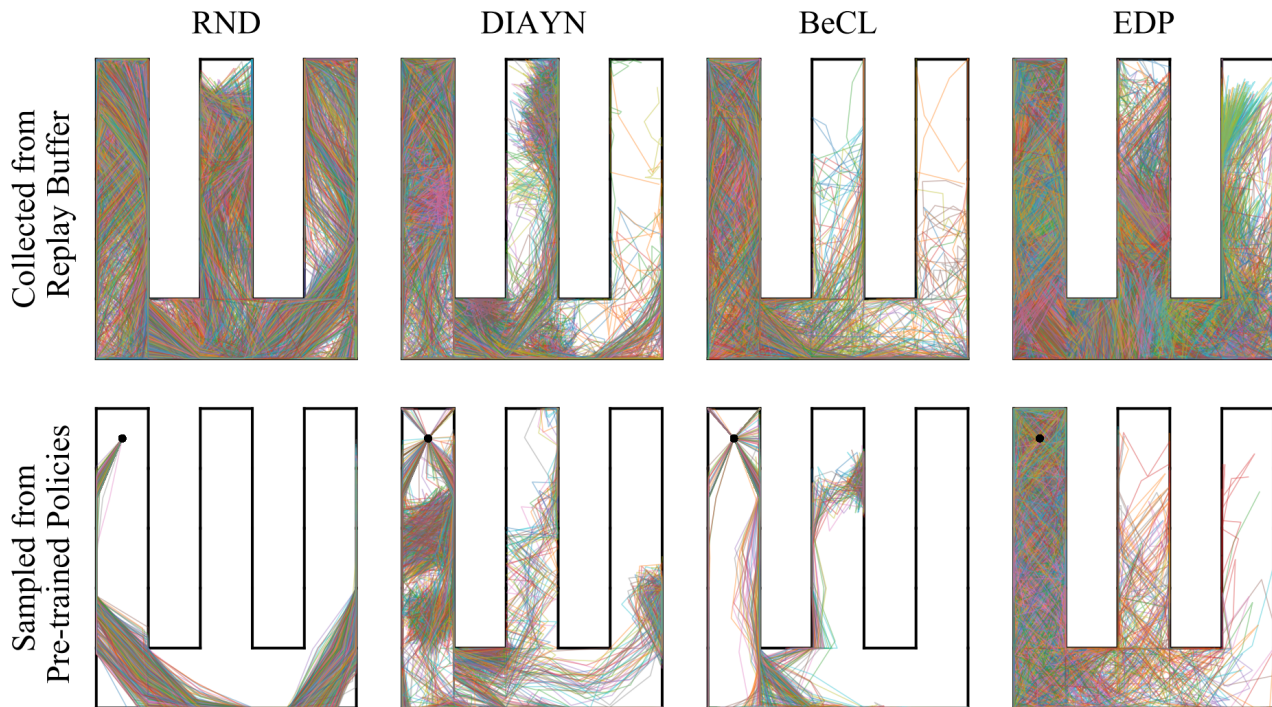


Figure 8. Visualization of different unsupervised RL pre-training methods in Square-c maze. The above part shows the trajectories in the replay buffer sampled by four algorithms during the unsupervised pre-training stage. The below part displays the trajectories directly sampled from the pre-trained policies of four algorithms.

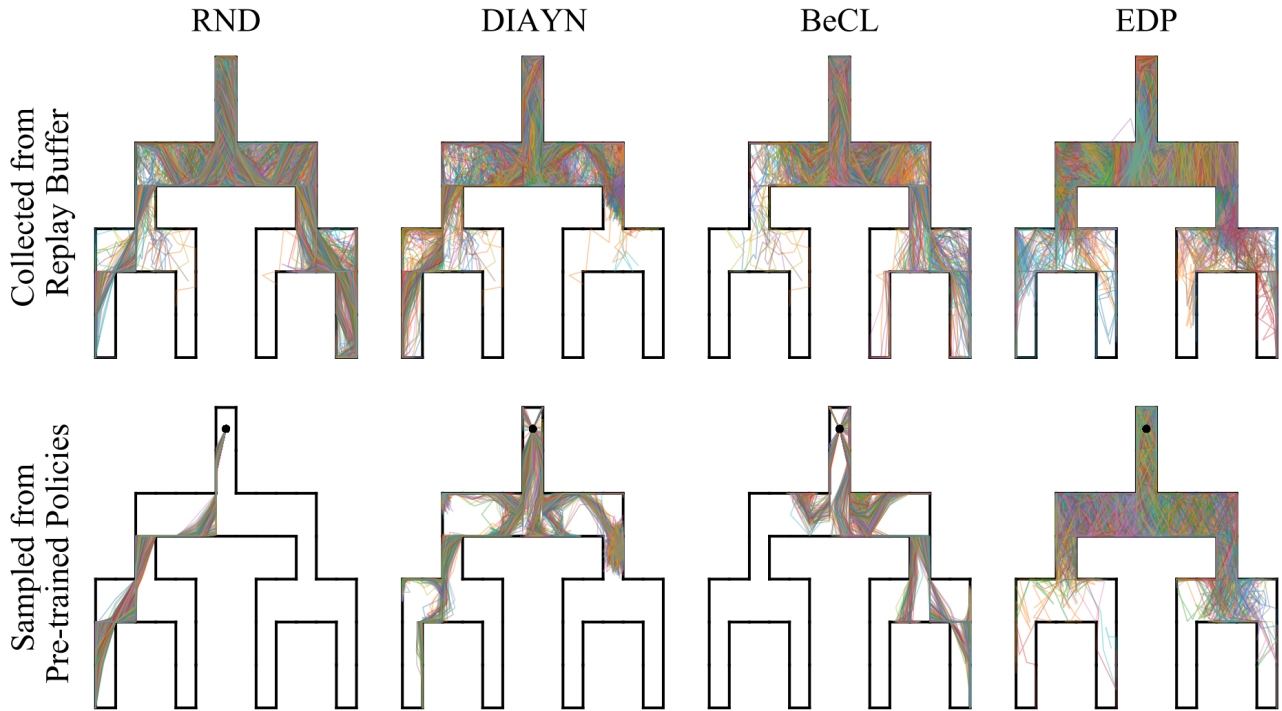


Figure 9. Visualization of different unsupervised RL pre-training methods in Square-tree maze. The above part shows the trajectories in the replay buffer sampled by four algorithms during the unsupervised pre-training stage. The below part displays the trajectories directly sampled from the pre-trained policies of four algorithms.

C.4. Additional Experiments in URLB

In Table 1, we report the detailed results of all methods in 4 downstream tasks of 4 domains in URLB. In both the Quadruped and Jaco domains, EDP obtains state-of-the-art performance in downstream tasks. Overall, there are the most number of downstream tasks that EDP performs the best and EDP significantly outperforms existing exploration algorithms.

Domains Tasks	Walker				Quadruped				Jaco				Hopper			
	stand	walk	run	flip	stand	walk	run	jump	tl	tr	bl	br	hop	hop-back	flip	flip-back
ICM	828.5	628.8	223.8	400.3	298.9	129.9	92.1	148.8	96.5	91.7	84.3	83.4	82.1	160.5	106.9	107.6
RND	878.3	745.4	348.0	454.1	792.0	544.5	447.2	612.0	98.7	110.3	107.0	105.2	83.3	267.2	132.5	184.0
Disagreement	749.5	521.9	210.5	340.1	560.8	382.3	361.9	427.9	142.5	135.1	129.6	118.1	86.2	255.6	113.0	215.3
LBS	594.9	603.2	138.8	375.3	413.0	253.2	203.8	366.6	166.5	153.8	129.6	139.6	24.8	240.2	88.9	105.6
DIAYN	721.7	488.3	186.9	317.0	640.8	525.1	275.1	567.8	29.7	15.6	30.4	38.6	1.7	10.8	0.7	0.5
SMM	914.3	709.6	347.4	442.7	223.9	93.8	91.6	96.2	57.8	30.1	34.8	45.0	29.3	61.4	47.0	29.7
LSD	770.2	532.3	167.1	309.7	319.4	186.3	179.6	283.5	11.6	33.6	22.5	6.7	12.0	6.6	2.9	12.2
CIC	941.1	883.1	399.0	687.2	789.1	587.8	475.1	630.6	148.8	168.9	122.3	145.9	82.7	191.6	96.2	161.3
BeCL	951.7	912.7	408.6	626.2	731.2	640.3	387.2	567.4	103.9	112.2	101.1	108.2	37.1	68.3	73.6	142.7
EDP (Ours)	942.1	761.5	272.1	427.0	920.7	749.6	464.9	705.9	179.7	167.8	133.8	117.1	89.5	233.5	113.4	185.5

Table 1. Detailed results in URLB. Average cumulative reward (mean of 10 seeds) of the best policy.